Atmospheric Environment 144 (2016) 60–68

Contents lists available at ScienceDirect

Atmospheric Environment

journal homepage: www.elsevier.com/locate/atmosenv

The importance of non-fossil sources in carbonaceous aerosols in a megacity of central China during the 2013 winter haze episode: A source apportionment constrained by radiocarbon and organic tracers

Junwen Liu [a, b], Jun Li [a, *], Matthias Vonwiller [b, c], Di Liu [a], Hairong Cheng [d], Kaijun Shen [a], Gary Salazar [b], Konstantinos Agrios [b, c], Yanlin Zhang [b, c, 1], Quanfu He [a], Xiang Ding [a], Guangcai Zhong [a], Xinming Wang [a], Sönke Szidat [b, **], Gan Zhang [a]

[a] State Key Laboratory of Organic Geochemistry, Guangzhou Institute of Geochemistry, Chinese Academy of Sciences, Guangzhou, 510640, China
[b] Department of Chemistry and Biochemistry & Oeschger Centre for Climate Change Research, University of Bern, Berne, 3012, Switzerland
[c] Laboratory of Radiochemistry, Paul Scherrer Institute, Villigen-PSI, 5232, Switzerland
[d] Department of Environmental Engineering, School of Resource and Environmental Science, Wuhan University, Wuhan, 430079, China

HIGHLIGHTS

- Radiocarbon and organic tracers were determined in a megacity of central China during an extreme haze event in 2013 winter.
- The contributions of non-fossil sources in OC and EC were 62% ± 5% and 26% ± 8%, respectively.
- The contributions of non-fossil sources in WIOC and WSOC were 61% ± 4% and 63% ± 6%, respectively.
- Most non-fossil SOC particles probably were derived from the atmospheric processes regarding biomass-burning.

ARTICLE INFO

Article history:
Received 7 June 2016
Received in revised form
22 August 2016
Accepted 23 August 2016
Available online 25 August 2016

Keywords:
Central China
Organic carbon
Elemental carbon
Radiocarbon
Organic tracer

ABSTRACT

To determine the causes of a severe haze episode in January 2013 in China, a source apportionment of different carbonaceous aerosols (CAs) was conducted in a megacity in central China (Wuhan, Hubei Province) by using the measurements of radiocarbon and molecular organic tracers. Non-fossil sources (e.g., domestic biofuel combustion and biogenic emissions) were found to be responsible for 62% ± 5% and 26% ± 8% of organic carbon (OC) and elemental carbon (EC) components by mass, respectively. Non-fossil sources contributed 57% ± 4% to total CAs in this large-scale haze event, whereas fossil-fuel sources were less dominant (43% ± 4%). The CAs were composed of secondary organic carbon (SOC; 46% ± 10%), primary fossil-fuel carbon (29% ± 4%) and primary biomass-burning carbon (25% ± 10%). Although SOC was formed mainly from non-fossil sources (70% ± 4%), the role of fossil precursors was substantial (30% ± 4%), much higher than at the global scale. Combined measurement of organic tracers and radiocarbon showed that most non-fossil SOC was probably derived from biomass burning during this long-lasting haze episode in central China.

1. Introduction

A severe and long-lasting haze episode, with an extremely elevated $PM_{2.5}$ (aerodynamic diameter ≤ 2.5 μm) concentration (the hourly concentration up to ~1000 μg/m^3) (Uno et al., 2014), occurred in January 2013 in central and eastern China. Because a high $PM_{2.5}$ loading can cause a reduction in visibility, climate changes, and human respiratory-cardiovascular diseases (Brunekreef and Holgate, 2002; Menon et al., 2002; Deng et al., 2008; Wang et al., 2014b), many concerns were raised by the public, government, and scientists. Numerous investigations have been performed to determine the characteristics of this air pollution crisis. He et al. (2014) identified a new haze formation mechanism regarding the conversion of SO_2 to sulfate, and reported that

* Corresponding author.
** Corresponding author.
E-mail addresses: junli@gig.ac.cn (J. Li), szidat@dcb.unibe.ch (S. Szidat).
[1] Now at Nanjing University of Information Science & Technology, Nanjing, 210044, China.

http://dx.doi.org/10.1016/j.atmosenv.2016.08.068
1352-2310/

the impact of motor vehicle on air quality was underestimated in the Beijing-Tianjin-Hebei Region. Using an aerodyne aerosol chemical speciation monitor, Sun et al. (2014) found that stagnant meteorological conditions, coal combustion, secondary production, and regional transport were the main factors leading to the formation of this haze in Beijing. Wang et al. (2014a) called on the government to establish a regional joint framework for mitigation of the severe air pollution based on their model evaluations. Currently, most of these studies have been conducted in northern China, specifically in Beijing, and have focused on the analysis of chemical concentrations. Measurements of more-specific-sources tracers (i.e., isotopes and organic tracers) during this haze period are still scarce.

Carbonaceous aerosols (CAs) are important major components of $PM_{2.5}$. However, CAs are poorly understood because of their vast number of emission sources, various physicochemical properties, and heterogeneous distribution in time and space. Total CAs values are generally expressed in terms of total carbon (TC), which contains organic carbon (OC) and elemental carbon (EC). EC is a primary carbon species that is derived solely from the incomplete combustion of carbon-containing materials. Ambient OC is a mixture of primary organic carbon (POC), which is emitted from various combustion processes, and secondary organic carbon (SOC), which is formed through the oxidation of volatile organic compounds (VOCs) (Pöschl, 2005; Calvo et al., 2013). In addition, a large fraction of SOC can be formed from the chemical reactions of POC (Robinson et al., 2007). OC can be further separated into water-soluble organic carbon (WSOC) and water-insoluble organic carbon (WIOC). These carbon particles in the atmosphere have two sources: fossil fuel (FF, e.g., from traffic exhaust, coal combustion, industry) and non-fossil (NF, e.g., from open/forest fire, biofuel burning, biogenic emission) emissions. Their unambiguous source apportionment has been conducted in recent years by the measurements of radiocarbon (^{14}C) (Gustafsson et al., 2009, Szidat et al., 2009; Chen et al., 2013; Liu et al., 2013; Huang et al., 2014; Liu et al., 2014; Zotter et al., 2014a; Andersson et al., 2015; Zhang et al., 2015). This radioisotope (half-life = 5730 years) enables a distinction between FF and NF sources because ^{14}C is absent in FF, but present at the current ambient level in NF materials. ^{14}C analyses of aerosols have seldom been reported in China due to the complexity of experimental procedures and the need for a specific analysis facility. Chen et al. (2013) first systematically investigated the ^{14}C signals of EC (or black carbon) in Beijing, Shanghai, and Xiamen, and found that 83–86% of EC was associated with FF combustion during the 2009–2010 winter, with the remainder derived from biomass burning (BB). Zhang et al. (2015) analyzed the ^{14}C levels of OC and EC in four Chinese cities—Beijing, Xi'an, Guangzhou, and Shanghai—and found that the contributions of FF sources to OC and EC were 35–49% and 57–80%, respectively, in January 2013. Andersson et al. (2015) found that during this haze period FF sources on average contributed 74%, 68% and 68% to EC in Beijing, Shanghai and Guangzhou, respectively. Liu et al. (2014) showed that the contribution of FF in OC and EC was 37% and 71% in Guangzhou during November 2012 to January 2013, respectively. A newly updated China emission inventory showed that the coal used in power plants is 8300 Gg, 28,000 Gg, 85,000 Gg, 80,000 Gg, 35,000 Gg, in Beijing (north China), Shanghai (east China), Guangdong (south China, the capital is Guangzhou), Shanxi (west China, the capital is Xi'an) and Hubei (central China, the capital is Wuhan), and the corresponding value for residential solid biomass is 880 Gg, 0 Gg, 22,000 Gg, 14,000 Gg and 26,000 Gg, respectively (Wang et al., 2012). These results indicate that biomass used for residential burning in Hubei seems higher than Guangdong, especially than Beijing and Shanghai. Given this difference of energy consumption pattern among different regions in China, the key sources of this haze episode probably is region-dependent. Previous ^{14}C-related studies also have displayed this difference. For example, the contribution of FF sources to OC in Beijing was 58% (Zhang et al., 2015), whereas it was <40% in Guangzhou on average (Liu et al., 2014; Zhang et al., 2015). Thus, this large-scale haze crisis was very likely caused by the convergence of materials from numerous point sources in regions with different sources. More ^{14}C-related studies are urgently needed to accurately and quantitatively elucidate the emission sources of CAs during such a regional haze crisis. On other hand, the sources of WSOC and WIOC differ markedly from those of EC (Liu et al., 2014). Thus, determination of the ^{14}C isotopic signals of various carbon species is necessary to obtain a better understanding of haze pollution characteristics and sources.

The haze phenomenon in China is very complex. First, Chinese cities are at the developmental stage of industrialization and urbanization, with a large demand for FF energy. Second, biofuel is a very common energy source in rural and suburban areas, in which ~50% of the Chinese population lives. Third, little is known about the evolution of SOC and its precursor VOCs, especially the relative contributions of FF and NF sources to SOC. Consequently, controversial results regarding the $PM_{2.5}$ sources in China have been published. One group reported that the annual contributions of coal and biomass combustion to $PM_{2.5}$ in Beijing were 7% and 6% (Zheng et al., 2005), respectively, whereas higher corresponding contributions (14–19% and 11–13%, respectively) have been reported in other studies (Song et al., 2006; Zhang et al., 2013a). This discrepancy are mainly due to the less-source-tracers such as K^+ and elements that needed to input into the models and their variable parameters. To determine the origins of haze particles, we measured ^{14}C isotopic signals and unique organic tracers in $PM_{2.5}$ samples with various levels in Wuhan (Fig. S1), the largest (~550 km^2) and most densely populated metropolis (~10 million) in central China. Wuhan is the capital of Hubei province and located in the core area of the January 2013 large-scale haze pollution (Fig. S1). According to the annual report of the Editorial Department of Wuhan Statistical Yearbook-2014, the gross domestic product was composed of agriculture (3.7%), industry (48.6%), and other sectors (47.7%). Although pollution is frequently severe in Wuhan, studies of air pollution in this megacity are only just beginning to occur. It should be noted that some ^{14}C-related studies have recently reported on aerosol sources of the haze episode in 2013 in other cities as we mentioned above, the important aspect of haze sources in the central China with a relatively high usage of biomass has not been addressed yet. Our study provides new insights into the sources of air pollution in Chinese city, specifically into the contributions of FF and NF sources to the different carbon species during this long and persistent haze incident in central China. We also conducted a source apportionment, including POC and SOC, through the combinational measurement of molecular markers and radiocarbon. To our best knowledge, this article is first to report on ^{14}C signals of CAs in this megacity.

2. Methods

2.1. Sample collection

In this study, ambient $PM_{2.5}$ sampling was conducted on the campus of Wuhan University (30.50°N, 114.35°N; 16 m above ground level) from 9 January to 6 February 2013 using a high-volume air sampler (1 m^3/min, XTrust Instruments, Shanghai, China) with a $PM_{2.5}$ inlet. No obvious point source was located in the vicinity of this site during the sampling campaign. Quartz fiber filters (QFFs) that had been pre-baked for 4 h at 450 °C were collected with 24-h resolution. After collection, the QFFs were

folded in half, wrapped in aluminum foil, sealed in air-tight plastic bags, and stored at −20 °C until analysis. This sampling site was able to characterize this regional haze episode in central China basing on the previous findings that the concentrations of submicron particles and the ionic compositions between the urban and suburban sites in Wuhan were very similar (Cheng et al., 2014).

2.2. Chemical analysis

Carbon species were measured using a thermal-optical carbon analyzer (Model 4L; Sunset Laboratory Inc., Tigard, OR, USA) with a non-dispersive infrared detector at the University of Bern, Switzerland, using the EUSAAR2 protocol (Cavalli et al., 2010). The repeatability (n = 5) of OC and EC determinations were 5% and 8% in this study. To minimize charring (Yu et al., 2002; Piazzalunga et al., 2011), determinations of WIOC and EC were made after water extraction (Zhang et al., 2012). Very little of EC would be lost during this water extraction (Zhang et al., 2012). The difference in TC values obtained with and without the water-extraction treatment was defined as WSOC. The BB tracers analyzed in this study were levoglucosan (Lev), galactosan (Gal), and mannosan (Man). Molecular tracers of secondary organic aerosols (SOAs) included six isoprene SOA tracers (*cis*-2-methyl-1,3,4-trihydroxy-1-butene; 3-methyl-2,3,4-trihydroxy-1-butene; *trans*-2-methyl-1,3,4-trihydroxy-1-butene; 2-methylglyceric acid; 2-methylthreitol; and 2-methylerythritol), two monoterpene SOA tracers (3-hydroxyglutaric acid, pinonic acid), one β-caryophyllene SOA tracer (β-carophyllene acid), and one aromatic SOA tracer (2,3-dihydroxy-4-oxopentanoic acid). Analytical procedures were described in detail in a previous study (Ding et al., 2012), and are provided in the Supporting Information. The relative standard deviation (RSD) for this reconstructed SOC in our lab was 51 ± 11% (Shen et al., 2015).

2.3. Radiocarbon analysis

Twelve samples (Table 1) with low to high $PM_{2.5}$ levels were selected for radiocarbon measurement. The ^{14}C measurements were conducted using an online system that couples the Sunset carbon analyzer with the MIni radioCArbon DAting System (MICADAS) (Agrios et al., 2015) at the Laboratory for the Analysis of Radiocarbon with AMS, University of Bern, Switzerland (Szidat et al., 2014). The separation of carbon species for ^{14}C analysis was undertaken with the Sunset OC/EC Analyzer following the Swiss_4S protocol (Zhang et al., 2012). All ^{14}C results were expressed as the fraction of modern (f_m) levels and corrected for decay between 1950 and the year of measurement. The degree of uncertainty in the ^{14}C measurements was in the range of 1–2%. Values of f_m for WSOC and TC were calculated from the isotopic mass conservation, and the f_m(OC) values reported here were corrected by a field blank (0.45 μg C/cm^2; $f_m = 0.61 \pm 0.02$). In this study, f_m was divided by the reference values (f_{ref}, representing the f_m value of pure NF OC and EC) and transformed into the fraction of contemporary (f_c, $f_c = f_m/f_{ref}$) levels to eliminate the effect of fallout from nuclear weapons testing (Levin et al., 2010). The f_{ref} values for OC (1.06 ± 0.05) and EC (1.10 ± 0.05) in 2013 were estimated based on a long-term time series of $^{14}CO_2$ at the Schauinsland station (Levin et al., 2010) and a tree-growth model (Mohn et al., 2008). The degree of uncertainty of f_c is generally <5%. The f_c value ranges from 0 to 1 and directly represents the NF contribution.

3. Results and discussion

3.1. Carbon composition pattern

All mass concentrations of $PM_{2.5}$ and carbon species are listed in Table 1. On average, 20% ± 3% (16–27%) of $PM_{2.5}$ in this study was explained by TC, which was within the range (14–40%) reported in other cities around the world (Pöschl, 2005; Ho et al., 2006; Cao et al., 2007; Zhao et al., 2013). A significant correlation was found between $PM_{2.5}$ and TC ($r = 0.84$, $p < 0.01$, Pearson, Two-tailed). As shown in Fig. S2, TC was composed of WIOC [47% ± 7%, RSD = 16%], followed by WSOC (39% ± 8%, RSD = 20%) and EC (14% ± 2%, RSD = 14%). WSOC thus had the largest RSD, which may reflect the complexity of sources as this carbon species contains many SOC components (Weber et al., 2007; Ding et al., 2008). EC was correlated significantly with OC ($r = 0.90$, $p < 0.01$, Pearson, Two-tailed), which suggests that they have common sources and atmospheric behaviors. However, we found that WIOC was correlated significantly with EC ($r = 0.91$, $p < 0.01$, Pearson, Two-tailed), whereas WSOC was not ($r = 0.55$, $p = 0.06$, Pearson, Two-tailed) (Fig. S3). This result confirms the previous findings that most ambient WIOC particles are directly emitted from sources (Miyazaki et al., 2006) and a large fraction of WSOC are derived by the atmospheric oxidation (Weber et al., 2007; Ding et al., 2008).

Table 1
Information of the samples selected for radiocarbon measurements.

Sampling date[a]	$PM_{2.5}$	WIOC	WSOC	OC	EC	TC	Levoglucosan	Mannosan	Galactosan
Jan.09	204	19.1	16.4	35.6	4.64	40.2	1083.00	57.22	33.03
Jan.10	214	20.9	16.7	37.6	6.86	44.5	1121.98	65.08	40.54
Jan.11	241	40.1	16.8	56.9	8.00	64.9	2113.08	131.52	69.85
Jan.12–16[b]	164–214								
Jan.17	149	9.70	11.4	21.1	3.60	24.7	352.28	19.49	11.56
Jan.18	153	16.2	7.61	23.8	5.06	28.9	553.82	37.28	19.08
Jan.19	143	13.4	9.78	23.2	3.62	26.8	690.11	38.47	20.27
Jan.20–25[b]	127–204								
Jan.26	227	16.8	17.0	33.8	4.96	38.8	694.07	31.01	20.40
Jan.27	257	20.5	16.1	36.6	5.72	42.3	927.44	52.07	31.06
Jan.28	191	16.4	17.6	34.0	4.93	38.9	918.92	55.67	31.72
Jan.29	122	10.4	16.0	26.4	4.19	30.6	806.75	43.97	26.26
Jan.30	124	10.3	12.0	22.3	4.37	26.7	940.87	55.07	26.56
Jan.31	88	10.4	6.05	16.4	3.59	20.0	1196.11	72.16	32.72
Feb.01–06[b]	43–124								

[a] The beginning date of sampling time. WIOC: water-insoluble organic carbon. WSOC: water-soluble organic carbon. OC: organic carbon. EC: elemental carbon. TC: total carbon.
[b] Days were not measured for chemicals and radiocarbon in this study. The units of $PM_{2.5}$, carbon species (WIOC, WSOC, OC, EC, and TC) and anhydrosugars (levoglucosan, mannosan, and galactosan) are μg/m^3,μg C/m^3 and ng/m^3, respectively.

3.2. Radiocarbon results

All percentage contributions of FF to the carbon species were <50%, with the exception of EC (Table 2), which implies that NF sources are very important in central China. The specific contributions of FF to WIOC, WSOC, OC, EC, and TC were 39% ± 4%, 37% ± 6%, 38% ± 5%, 74% ± 8%, and 43% ± 4%, respectively. No significant correlation (i.e. $0.80 > p > 0.50$, Pearson, Two-tailed) was found between the concentrations of carbon species and their corresponding ^{14}C levels (Table S1). These results imply that this large-scale haze event in China was not caused simply by only one type of emission source.

Table 3 shows ^{14}C-derived source apportionments from other urban and background regions around the world. The contributions of FF sources to all carbon species were greater at urban sites than at background locations. If we take the ^{14}C level in the natural conservation area of Hainan, China, as a reference for pristine air, ~20–30% greater contributions from FF sources among the carbon species were observed in this study. Large contributions from FF sources were also found in Ningbo, China, another background location. This result was obtained because Ningbo station can be significantly impacted by the polluted air masses originating from the Beijing-Tianjin-Hebei city agglomeration (Liu et al., 2013). The FF contribution (38% ± 5%) to OC in this study was similar to those in Guangzhou (37% ± 4%), Amsterdam (36% ± 17%), Göteborg (38% ± 4%), and Pasadena (42% ± 15%), but higher than contributions measured in some European cities, such as Bern (30%) and Zürich (16%). Similar results were observed for WIOC and EC. The ^{14}C signals of WIOC, EC, and OC in Wuhan did not differ distinctly from those of other cities in developed countries. This finding was unexpected because FFs are used extensively in Chinese megacities due to the large amounts of vehicles and industry. The most likely explanation is that intensive and extensive BB occurred during the haze period. This interpretation is supported by the extremely high levels of BB tracers. In this study, Lev concentrations were 0.352–2.113 μg/m^3 (0.950 ± 0.421 μg/m^3; Table 1), which was higher than in samples collected during a period of severe BB incidents (0.310–1.080 μg/m^3, Taiwan, rice straw burning, December 2006) (Lee et al., 2008) and ~10–100 times higher than in the clean air of European cities (e.g., Göteborg, Sweden; 0.01–0.07 μg/m^3) (Szidat et al., 2009). In addition, very few wild fires were observed during the sampling campaign (Fig. S4), indicating that BB activity occurred indoors (i.e., domestic heating and cooking) that could not be detected by satellite. FF contributions to WSOC were higher in Wuhan (37% ± 6%) than in two other cities in China, i.e., Xi'an (31%) and Guangzhou (33% ± 3%), and also higher than in cities with good air quality; for example, Göteborg (23–26%), Sapporo (16%), Zürich (5–14%), and Bern (14%, Table 3). Generally, WSOC is considered to be a mixture of SOC and BB-derived POC (Weber et al., 2007; Ding et al., 2008). Therefore, a larger contribution of FF source to WSOC indicates that a larger amount of FF-derived VOCs was involved in SOC formation.

Table 2
Relative contribution of fossil fuel sources to different carbon fractions (%).

Sampling time	WIOC	WSOC	OC	EC	TC
Jan.09	39 ± 3	35 ± 4	37 ± 3	81 ± 2	42 ± 4
Jan.10	38 ± 3	38 ± 4	38 ± 3	77 ± 1	44 ± 3
Jan.11	37 ± 3	39 ± 5	38 ± 3	79 ± 2	43 ± 4
Jan.17	48 ± 3	45 ± 3	46 ± 3	76 ± 2	41 ± 3
Jan.18	38 ± 3	41 ± 5	39 ± 3	81 ± 1	46 ± 3
Jan.19	36 ± 3	35 ± 4	36 ± 3	87 ± 1	43 ± 3
Jan.26	44 ± 3	43 ± 4	43 ± 3	70 ± 2	47 ± 3
Jan.27	41 ± 3	44 ± 4	42 ± 3	74 ± 1	46 ± 3
Jan.28	41 ± 3	39 ± 4	40 ± 3	74 ± 1	44 ± 3
Jan.29	37 ± 3	30 ± 4	32 ± 3	64 ± 2	37 ± 4
Jan.30	34 ± 3	23 ± 5	28 ± 4	58 ± 2	37 ± 4
Jan.31	37 ± 3	34 ± 5	36 ± 3	67 ± 2	41 ± 4
Average	39 ± 4	37 ± 6	38 ± 5	74 ± 8	43 ± 4

3.3. Secondary organic carbon: non-fossil versus fossil sources

A source-apportionment method for OC, including primary and secondary sources, was implemented using the measured carbon fractions, anhydrosugars, and ^{14}C isotopic signals. OC can be divided into fossil OC (OC_f) and non-fossil OC (OC_{nf}) based on the ^{14}C measurement. OC_{nf} consists of BB-derived primary OC (OC_{bb_pri}), NF-derived SOC (OC_{nf_sec}), and biological primary carbon (BPC), such as spore and plant debris. Atmospheric BPC exists mainly in the coarse mode (>2.5 μm) and accounts for ~1% of OC in $PM_{2.5}$ (Guo et al., 2012). Thus, this carbon species was not considered in this study. OC_{bb_pri} was estimated semi-quantitatively from Lev concentrations due to its unique origin from BB:

$$OC_{bb\_pri} = Lev \times (OC/Lev)_{bb} \quad (1)$$

The ratio of OC to Lev obtained from a BB emission inventory [$(OC/Lev)_{bb}$] depends significantly on the types of biomass. The composition of anhydrosugars (Gal, Man, and Lev) provides diagnostic information regarding the type of biomass (Sang et al., 2012). In this study, anhydrosugars were composed primarily of Lev (92% ± 0.6%), with the rest being Man (5% ± 0.5%) and Gal (3% ± 0.2%). Such stable (RSD < 10%) composition profiles reflect a predominant type of biomass. In general, hardwood (Lev/Man = 22 ± 9; Man/Gal = 3 ± 2), softwood (Lev/Man = 5 ± 1; Man/Gal = 6 ± 3), and annual plant (Lev/Man = 28 ± 15; Man/Gal = 0.6 ± 0.3) are the three most important types of biomass (Liu et al., 2014). According to the ratios of Lev/Man (18 ± 2) and Man/Gal (2 ± 0.2) obtained in this study, 7.76 ± 1.47 was adopted for the $(OC/Lev)_{bb}$, which is the typical emission factor of hardwood (Liu et al., 2014).

Thus, we estimated the fraction of OC_{nf_sec} through subtraction:

$$OC_{nf\_sec} = OC_{nf} - OC_{bb\_pri} \quad (2)$$

In principle, fresh primary OC emitted from FF combustion is water-insoluble. After analyzing the differences in WSOC levels at sites with no direct influence from vehicle exhaust emissions. Weber et al. (2007) concluded that primary WSOC emitted directly by vehicles is very limited. With regard to coal, another type of FF, only ~1% of fresh OC is water-soluble (Park et al., 2012). Thus, POC derived from FF combustion can reasonably be considered to be water-insoluble. WSOC is used to estimate levels of SOC in the absence of BB emissions (Weber et al., 2007), which means that FF-derived SOC is water-soluble. Some studies have shown that WIOC can also be partially formed through FF-derived VOCs in Egypt (Favez et al., 2008). Since the formation and evolution of SOC is a continuous aging process (Robinson et al., 2007; Kroll and Seinfel, 2008), this "FF-derived water-insoluble SOC" probably can be attributed to the less oxidation degree during a short time in an arid atmosphere. Furthermore, these SOC calculations were based on the method of minimum ratio of OC-to-EC, which will certainly overestimate the SOC loading when the atmosphere is impacted by the BB plumes (Ding et al., 2012). Consequently, in 24-h samples, the use of FF-derived WSOC ($WSOC_f$) and FF-derived WIOC ($WIOC_f$) as proxies for the estimation of SOC (OC_{f_sec}) and POC (OC_{f_pri}), respectively, would be feasible and reasonable. The typical degree of uncertainty for these POC and SOC calculations is 20–25% (Zhang et al., 2015). This method has been used widely in previous studies performed in urban and background locations (Liu et al., 2014; Zhang et al., 2014a). Thus, FF-derived POC and SOC could be

Table 3
Relative fossil fuel source contributions (%) to carbon fractions around the world.

	Location	Year	Season	WIOC	WSOC	OC	EC	TC	Size	References
Urban	Lhasa, China	2006/2007	Annual	–	–	–	–	51 ± 10	TSP	(Huang et al., 2010)
Urban	Shanghai, China	2013	Winter	–	–	49 ± 2	79 ± 4	–	$PM_{2.5}$	(Zhang et al., 2015)
Urban	Beijing, China	2009/2010	Winter	–	–	–	83 ± 4	–	$PM_{2.5}$	(Chen et al., 2013)
Urban	Beijing, China	2001	Annual	–	–	–	–	60 ± 5	$PM_{2.5}$	(Yang et al., 2005)
Urban	Beijing, China	2013	Winter			58 ± 5	76 ± 4	–	$PM_{2.5}$	(Zhang et al., 2015)
Urban	Guangzhou, China	2012/2013	Winter	40 ± 6	33 ± 3	37 ± 4	71 ± 10	42 ± 7	$PM_{2.5}$	(Liu et al., 2014)
Urban	Guangzhou, China	2011	Winter	53	29	42	–	–	PM_{10}	(Zhang et al., 2014b)
Urban	Guangzhou, China	2013	Winter			35 ± 8	69	–	$PM_{2.5}$	(Zhang et al., 2015)
Urban	Xi'an, China	2009	Autumn	–	31	–	–	49	$PM_{2.5}$	(Pavuluri et al., 2013)
Urban	Xi'an, China	2013	Winter			37 ± 3	78 ± 3	–	$PM_{2.5}$	(Zhang et al., 2015)
Urban	Wuhan, China	2013	Winter	39 ± 4	37 ± 6	38 ± 5	74 ± 8	43 ± 4	$PM_{2.5}$	this work
Urban	Sapporo, Japan	2010	Summer	–	16	–	–	46	$PM_{3.0}$	(Pavuluri et al., 2013)
Urban	Amsterdam, The Netherlands	2006	Jan–Jun	–[a]	–	36 ± 17	–	–	PM_{10}	(Dusek et al., 2013)
Urban	Göteborg, Sweden	2005	Winter	52 ± 10	23 ± 9	38 ± 4	89 ± 3	–	$PM_{2.5}$	(Szidat et al., 2009)
Urban	Göteborg, Sweden	2006	Summer	34 ± 2	26 ± 4	24 ± 3	85 ± 2	–	$PM_{2.5}$	(Szidat et al., 2009)[b]
Urban	Zürich, Switzerland	2002	Summer	39 ± 5	14 ± 8	25 ± 7	70 ± 1	37 ± 3	PM_{10}	(Szidat et al., 2004)
Urban	Zürich, Switzerland	2008	Winter	28	5	16	66	–	PM_{10}	(Zhang et al., 2013b)
Urban	Bern, Switzerland	2009	Winter	37	14	30	–	–	PM_{10}	(Zhang et al., 2014b)
Urban	Washington, U.S.	2004/2005	Annual	–	–	–	–	50	$PM_{2.5}$	(Schichtel et al., 2008)
Urban	Pasadena, U.S.	2010	Summer	–	–	42 ± 15	–	49 ± 15	$PM_{1.0}$	(Zotter et al., 2014b)
Background	Ningbo, China	2009/2010	Annual	40 ± 7	–	–	77 ± 12	–	$PM_{2.5}$	(Liu et al., 2013)
Background	Hainan, China	2005/2006	Annual	17 ± 10	18 ± 13	19 ± 10	38 ± 11	23 ± 10	$PM_{2.5}$	(Zhang et al., 2014a)
Background	Hanimaadhoo, Maldives	2006/2008/2009	Winter	–	17 ± 4	–	59	32	TSP	(Gustafsson et al., 2009; Kirillova et al., 2013)
Background	Sinhagad, India	2006/2008/2009	Winter	–	23 ± 4	–	46	35	TSP	(Gustafsson et al., 2009; Kirillova et al., 2013)
Background	Petten, The Netherlands	2009	Summer	–	–	19 ± 13	–	–	TSP	(Dusek et al., 2013)
Background	Grand Canyon, U.S.	2005/2006	Winter	–	–	–	–	0	$PM_{2.5}$	(Schichtel et al., 2008)
Background	Jeju Island, Korea	2011	Summer	–	30–50	–	–	–	$TSP/PM_{2.5}$	(Kirillova et al., 2014)

[a] Data are not reported. WIOC: water-insoluble organic carbon; WSOC: water-soluble organic carbon; OC: organic carbon; EC: elemental carbon; TC: total carbon.
[b] An abnormal sample was not included.

estimated as follows:

$$OC_{f\_pri} = WIOC \times (1 - f_c) \quad (3)$$

and

$$OC_{f\_sec} = WSOC \times (1 - f_c) \quad (4)$$

Source apportionment was achieved according to the approaches described above (Fig. 1). The total contribution of primary FF sources ($EC_f + OC_{f\_pri}$, 29% ± 4%) was only ~4% greater than the total contribution of primary BB sources ($EC_{bb} + OC_{bb\_pri}$, 25% ± 10%), indicating the importance of BB in this strong haze episode. The largest contributor was SOC, which accounted for 46% ± 10% of TC. Considering all carbon species, OC_{nf_sec} (32% ± 8%) contributed most to TC, followed by OC_{bb_pri} (21% ± 9%), OC_{f_pri} (18% ± 3%), OC_{f_sec} (14% ± 3%), EC_f (11% ± 2%), and EC_{bb} (4% ± 1%). The average percentage of total SOC in OC in this study (54% ± 11%) was similar to the values reported in other studies conducted during the same haze period and obtained using the high-resolution aerosol mass spectrometer: 41–59% (Sun et al., 2014) and 44–71% (Huang et al., 2014) from online and offline measurements, respectively.

Highly stable ratios of SOC/OC (57% ± 5%) and OC_{f_sec}/SOC (30% ± 4%) were found in samples collected during the most polluted days, with $PM_{2.5}$ concentrations >100 μg/m^3 (Fig. 2), indicating that a dynamic balance of the VOCs-to-SOC conversion system or aging processes was achieved for FF-derived and NF-derived SOC during this long-lasting haze period. In other words, SOC/OC ratios were already independent of the severity of air pollution due to the depletion of atmospheric oxidants and their reactive capacity during this haze period; thus, the increase in TC/$PM_{2.5}$ particles was correlated more with primary emissions. This result is confirmed by previous studies that the percentage of SOC in OC is relatively stable in the heavily polluted days with high $PM_{2.5}$ level but much higher than that in less polluted days with low $PM_{2.5}$ level (Huang et al., 2014), and the concentration of OH radicals in winter haze days (0.34×10^6 molec cm^{-3}) is only ~35% of that in winter non-haze days (0.99×10^6 molec cm^{-3}) (Rao et al., 2016). A much lower value of 20% was observed for SOC/OC on 31 January due to the removal of pollutants by precipitation and the presence of relatively clean air masses from southern areas (Fig. S1), which conversely implies that the SOC/OC ratio could increase by a factor of ~3 during the process of haze formation (from less polluted to severely polluted days) and related aerosol aging. This result shows that secondary formation is a vital factor in the control of large-scale haze formation, with low to high $PM_{2.5}$ loadings. The proportional content of OC_{f_sec} in SOC on 31 January was 62%, which was twice as high as that on highly polluted days (30% ± 4%). Because rainfall cleared the well-established haze system, the higher ratio of OC_{f_sec}/SOC observed on 31 January may reflect faster reaction rates of FF-derived VOCs than NF-derived VOCs or the close proximity of fossil VOC emissions to the sampling site. However, the proportional content of OC_{f_sec} in SOC (32% ± 10%) obtained in this study was 2–3 times higher than in areas with good air quality in developed countries, such as Puy de Dôme, France (12–14%) and Schauinsland, Germany (7–16%) (Gelencsér et al., 2007).

3.4. Non-fossil SOC: biomass burning versus biogenic emission emissions

Atmospheric NF SOC (OC_{nf_sec}) has two main origins: BB (OC_{bb_sec}) and biogenic emissions (OC_{bio_sec}). Much of our knowledge of tracer derived-SOC (SOC_T) has been obtained through

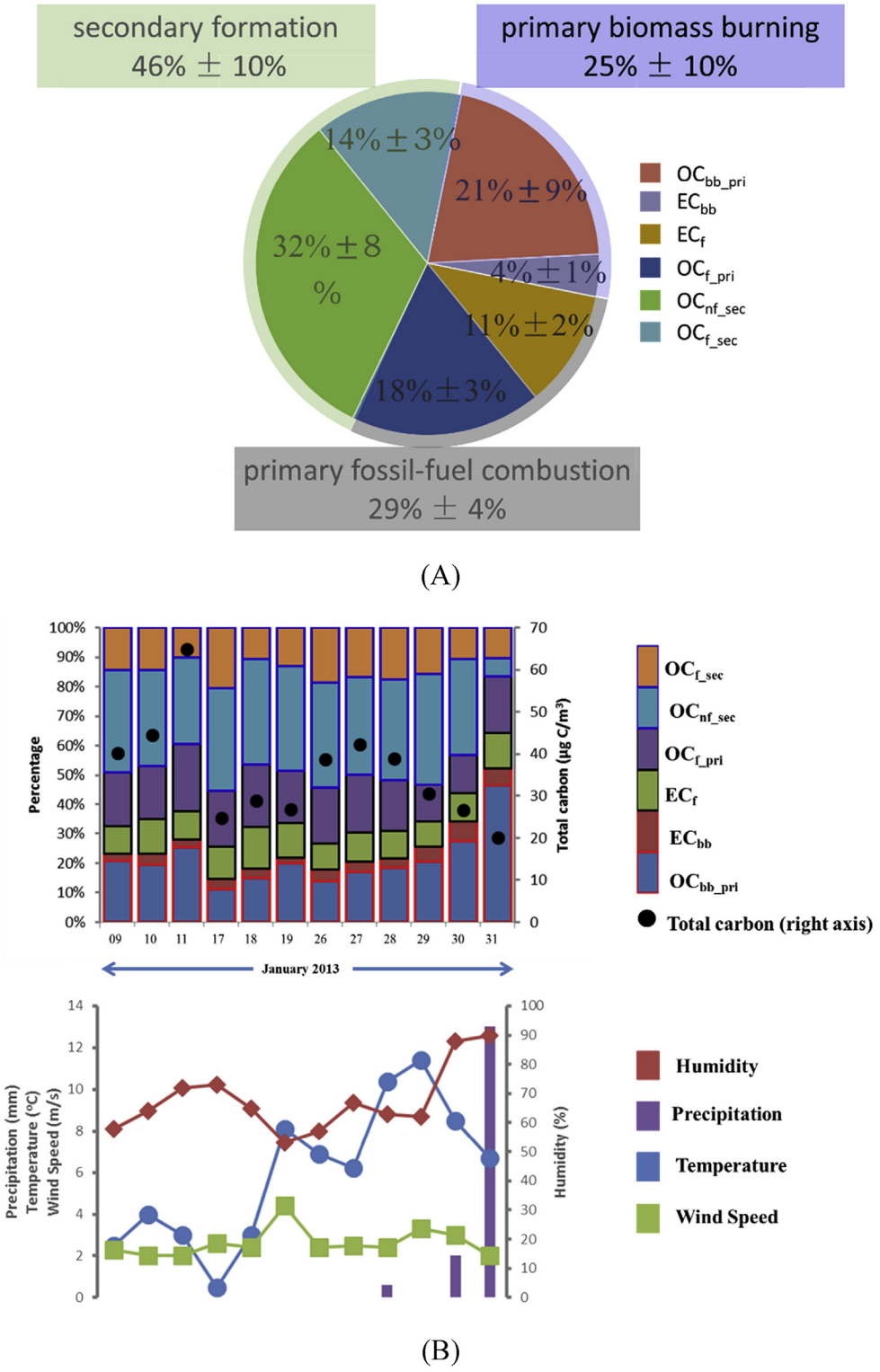

Fig. 1. Total carbon composition patterns regarding emission sources and carbon species. (A): average (n = 12); (B): individual samples and the meteorological parameters.

measurements performed in the field and in smog chambers. In general, monoterpene, isoprene, β-carophyllene, and aromatics are the most important precursor VOCs for atmospheric reactions. Kleindienst et al. (2007) found that the content of SOC_T in OC was in the range of 18–69% in North Carolina, with the lower values in winter and the higher values in summer. Studies conducted in the Midwestern US have documented similar levels (17–53%) (Lewandowski et al., 2008), implying that most SOC can be identified by these tracers. For China, however, substantially less SOC has been identified using these organic tracers: only 10–40% of OC has been apportioned by SOC_T in the summer (Hu et al., 2008; Fu et al., 2010; Ding et al., 2012; Guo et al., 2012; Feng et al., 2013),

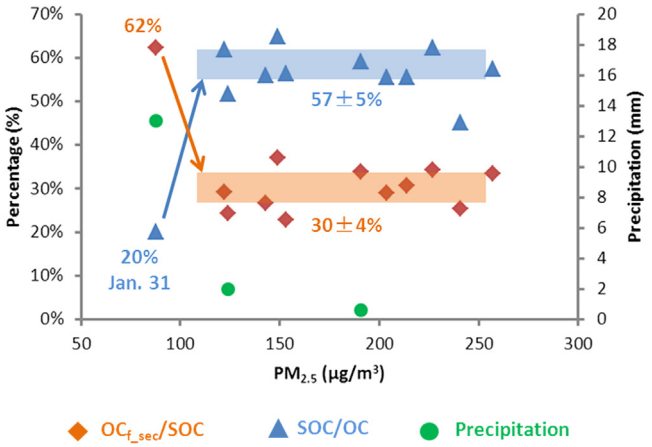

Fig. 2. Percentages of secondary organic carbon (SOC) in organic carbon (OC) and fossil fuel-derived SOC (OC_{f_sec}) in SOC with the increase of $PM_{2.5}$ concentrations.

~30–40% lower than found in studies performed in developed countries. Particularly in winter, a season with more BB activities, SOC_T merely accounted for <10% of OC and <1% of OC in southern (Ding et al., 2012) and eastern China (Feng et al., 2013), respectively. These results can likely be explained by the inability of the SOC_T method to estimate the SOC formed by the VOCs released by BB and aging processes, which are probably the critical formation pathways of SOC in Chinese cities. Concentrations of the measured SOC tracers from 26 to 31 January are shown in Table 4. The most abundant of measured tracers was 3-hydroxyglutaric acid, an oxidation product of monoterpene, with an average concentration of 12.2 ± 4.56 ng/m^3, followed by β-carophyllene acid (5.76 ± 2.45 ng/m^3), 2,3-dihydroxy-4-oxopentanoic acid (4.57 ± 1.96 ng/m^3), pinonic acid (3.54 ± 3.22 ng/m^3), 2-methylglyceric acid (1.89 ± 0.66 ng/m^3), and *trans*-2-methyl-1,3,4-trihydroxy-1-butene (1.82 ± 1.12 ng/m^3). The remaining compounds were present at levels of <1 ng/m^3. These concentrations are in agreement with those reported in previous studies performed in winter (Kleindienst et al., 2007; Ding et al., 2012; Feng et al., 2013). The largest contributors to SOC_T in this study were aromatic compounds (52% ± 8%; Fig. S5); this value is in line with that obtained in an investigation performed in Shanghai, China (58–65%) (Feng et al., 2013), but much higher than reported in developed regions in the US (18%) (Kleindienst et al., 2007). As mentioned above, a large amount of SOC in China appears to be missing from calculations based on tracers, with only 1.6–5.5% of OC identified by SOC_T in this study, which is similar to values reported in previous studies conducted in China (Ding et al., 2012; Feng et al., 2013). As suggested above, BB probably makes a large contribution to SOC in China. Reports have suggested that 25–50% of VOCs in China originate from BB (Bo et al., 2008; Liu et al., 2008b). However, to our knowledge, the direct quantification of ambient BB-derived SOC (SOC_{bb}) has not been achieved, due to the limited number of chamber experiments involving BB. In this study, a rough estimation of SOC_{bb} ($SOC_{bb} = OC_{nf\_sec} - SOC_{bio}$) was obtained based on the combination of ^{14}C and molecular markers of biogenic emissions (Table S2). It should be noted that some biogenic VOCs such as isoprene may can be emitted by BB but its concentration and relative contribution in total BB-derived VOCs is extremely low (Liu et al., 2008a) and can be ignored in this study. The results showed that almost all (93–98%) OC_{nf_sec} was due to SOC_{bb}, with the exception of the sample collected on the day when it rained (31 January, 70%). These results show a significantly dominant influence of BB on OC_{nf_sec} during this long-lasting winter haze, corresponding to the very low levels of biogenic VOCs in winter. Because few studies have quantified ambient SOC_{bb}, direct comparison of our results with those of other studies is difficult. However, using the proton nuclear magnetic resonance spectroscopy, high resolution–time of flight–aerosol mass spectrometry, and ^{14}C analysis, a recent study found that 73–100% of oxidized OC was derived from NF sources during a period with limited biogenic emissions in Italy (Paglione et al., 2014). These preliminary results demonstrate the greater importance of BB than biogenic emissions on SOC during winter. Because the conversion factors of SOA tracers to their corresponding SOC values are significantly depending on the chamber parameters, a large amount of uncertainty exists for the calculation of SOC_{bio} and the SOC_{bb} values reported in this study. More exploratory work is required to obtain further insights into the quantitation of SOC derived from BB, which will greatly enhance our knowledge of atmospheric reactions and the control of air pollution.

4. Conclusion

The haze occurred in 2013 winter was an unprecedented air pollution crisis in China. Carbonaceous aerosols play an important and critical role in the formation and evolution of the haze phenomenon but is still poorly constrained on their emission sources. In this study, radiocarbon was employed to identify the relative contributions of fossil (e.g., traffic and industry) and non-fossil (e.g., forest fire, biogenic emission and the burning of agricultural residues) sources in various carbon species in $PM_{2.5}$ of Wuhan, the largest city in central China, during this severe haze episode. Biomass burning contributed 26% ± 8% of elemental carbon (EC) with the rest coming from fossil sources (74% ± 8%). Higher contributions of non-fossil sources were observed in two organic carbon (OC) species: 61% ± 4% in water-insoluble organic carbon (WIOC) and 63% ± 6% in water-soluble organic carbon (WSOC),

Table 4
Concentrations (ng/m^3) for monoterpene, isoprene, β-carophyllenene and aromatic tracer compounds observed at Wuhan (central China) in winter.

		Jan.26	Jan.27	Jan.28	Jan.29	Jan.30	Jan.31	Average	Std. dev.
Monoterpene Tracers	3-hydroxyglutaric acid	4.79	16.0	16.3	14.3	14.8	6.82	12.2	4.58
	pinonic acid	1.48	5.71	9.72	2.53	0.66	1.14	3.54	3.22
	Total	6.28	21.7	26.0	16.8	15.4	7.96	15.7	6.98
Isoprene Tracers	*cis*-2-methyl-1,3,4-trihydroxy-1-butene	0.16	0.44	0.91	1.04	0.45	0.51	0.59	0.30
	3-methyl-2,3,4-trihydroxy-1-butene	0.17	0.28	0.27	0.46	0.20	0.21	0.27	0.10
	trans-2-methyl-1,3,4-trihydroxy-1-butene	0.76	0.75	3.42	3.29	1.47	1.20	1.82	1.12
	2-methylglyceric acid	1.35	2.68	2.66	2.26	1.18	1.20	1.89	0.66
	2-methylthreitol	0.49	1.20	0.98	0.90	0.57	0.61	0.79	0.25
	2-methylerythritol	1.03	2.35	2.44	2.03	1.18	1.60	1.77	0.54
	Total	3.96	7.69	10.7	9.99	5.05	5.34	7.12	2.54
β-Carophyllene Tracer	β-carophyllene acid	2.22	6.09	10.12	4.13	6.91	5.11	5.76	2.45
Aromatic tracer	2,3-dihydroxy-4-oxopentanoic acid	2.43	5.62	7.69	5.93	2.66	3.07	4.57	1.97

respectively. The levoglucosan mass concentration was up to 0.35–2.1 μg/m^3. These results suggest that biomass burning is an important driver for the haze phenomenon in Chinese cities, which probably because the burning of biofuel is still very extensive in China, especially in winter season. Combined with the measurements of secondary organic tracers, we inferred in this study that a vast majority of secondary organic carbon (SOC) in this event were derived from the atmospheric processes that related with biomass burning.

Acknowledgements

This work was supported by the "Strategic Priority Research Program (B)" of the Chinese Academy of Sciences (grant no. XDB05040503), the Natural Science Foundation of China (grant nos. 41430645, 41473101 and 41373131), Guangzhou Science and Technology Plan Project (grant no. 201504010002) and the Guangzhou Elites Scholarship Council (no. JY201332). The authors gratefully acknowledge the National Oceanic and Atmospheric Air Resources Laboratory for the provision of the HYSPLIT transport and dispersion model and the moderate-resolution imaging spectroradiometer mission scientists and associated NASA personnel for the AOD data. This is a contribution of GIGCAS (No. IS-2290).

Appendix A. Supplementary data

Supplementary data related to this article can be found at http://dx.doi.org/10.1016/j.atmosenv.2016.08.068.

References

Agrios, K., Salazar, G., Zhang, Y.-L., Uglietti, C., Battaglia, M., Luginbühl, M., Ciobanu, V.G., Vonwiller, M., Szidat, S., 2015. Online coupling of pure O_2 thermo-optical methods–^{14}C AMS for source apportionment of carbonaceous aerosols. Nucl. Instrum. Methods Phys. Res. Sect. B Beam Interact. Mater. Atoms 361, 288–293.

Andersson, A., Deng, J., Du, K., Zheng, M., Yan, C., Sköld, M., Örjan, G., 2015. Regionally-varying combustion sources of the January 2013 severe haze events over eastern China. Environ. Sci. Technol. 49 (4), 2038–2043.

Bo, Y., Cai, H., Xie, S., 2008. Spatial and temporal variation of historical anthropogenic NMVOCs emission inventories in China. Atmos. Chem. Phys. 8 (23), 7297–7316.

Brunekreef, B., Holgate, S.T., 2002. Air pollution and health. Lancet 360 (9341), 1233–1242.

Calvo, A., Alves, C., Castro, A., Pont, V., Vicente, A., Fraile, R., 2013. Research on aerosol sources and chemical composition: past, current and emerging issues. Atmos. Res. 120, 1–28.

Cao, J.J., Lee, S.C., Chow, J.C., Watson, J.G., Ho, K.F., Zhang, R.J., Jin, Z.D., Shen, Z.X., Chen, G.C., Kang, Y.M., Zou, S.C., Zhang, L.Z., Qi, S.H., Dai, M.H., Cheng, Y., Hu, K., 2007. Spatial and seasonal distributions of carbonaceous aerosols over China. J. Geophys. Res. Atmos. 112, D22S11.

Cavalli, F., Viana, M., Yttri, K., Genberg, J., Putaud, J.-P., 2010. Toward a standardised thermal-optical protocol for measuring atmospheric organic and elemental carbon: the EUSAAR protocol. Atmos. Meas. Tech. 3 (1), 79–89.

Chen, B., Andersson, A., Lee, M., Kirillova, E.N., Xiao, Q., Krusa, M., Shi, M., Hu, K., Lu, Z., Streets, D.G., Du, K., Gustafsson, Ö., 2013. Source forensics of black carbon aerosols from China. Environ. Sci. Technol. 47 (16), 9102–9108.

Cheng, H., Gong, W., Wang, Z., Zhang, F., Wang, X., Lv, X., Liu, J., Fu, X., Zhang, G., 2014. Ionic composition of submicron particles (PM 1.0) during the long-lasting haze period in January 2013 in Wuhan, central China. J. Environ. Sci. 26 (4), 810–817.

Deng, X., Tie, X., Wu, D., Zhou, X., Bi, X., Tan, H., Li, F., Jiang, C., 2008. Long-term trend of visibility and its characterizations in the Pearl River Delta (PRD) region, China. Atmos. Environ. 42 (7), 1424–1435.

Ding, X., Zheng, M., Yu, L., Zhang, X., Weber, R.J., Yan, B., Russell, A.G., Edgerton, E.S., Wang, X., 2008. Spatial and seasonal trends in biogenic secondary organic aerosol tracers and water-soluble organic carbon in the southeastern United States. Environ. Sci. Technol. 42 (14), 5171–5176.

Ding, X., Wang, X.M., Gao, B., Fu, X.X., He, Q.F., Zhao, X.Y., Yu, J.Z., Zheng, M., 2012. Tracer-based estimation of secondary organic carbon in the Pearl River Delta, south China. J. Geophys. Res. Atmos. 117, D05313.

Dusek, U., Brink, H.M., Meijer, H.A.J., Kos, G., Mrozek, D., Röckmann, T., Holzinger, R., Weijers, E.P., 2013. The contribution of fossil sources to the organic aerosols in the Netherlands. Atmos. Environ. 74, 169–176.

Favez, O., Sciare, J., Cachier, H., Alfaro, S.C., Abdelwahab, M.M., 2008. Significant formation of water-insoluble secondary organic aerosols in semi-arid urban environment. Geophys. Res. Lett. 35, L15801.

Feng, J., Li, M., Zhang, P., Gong, S., Zhong, M., Wu, M., Zheng, M., Chen, C., Wang, H., Lou, S., 2013. Investigation of the sources and seasonal variations of secondary organic aerosols in $PM_{2.5}$ in Shanghai with organic tracers. Atmos. Environ. 79, 614–622.

Fu, P., Kawamura, K., Kanaya, Y., Wang, Z., 2010. Contributions of biogenic volatile organic compounds to the formation of secondary organic aerosols over Mt. Tai, central east China. Atmos. Environ. 44 (38), 4817–4826.

Gelencsér, A., May, B., Simpson, D., Sánchez-Ochoa, A., Kasper-Giebl, A., Puxbaum, H., Caseiro, A., Pio, C., Legrand, M., 2007. Source apportionment of PM2.5 organic aerosol over Europe: primary/secondary, natural/anthropogenic, and fossil/biogenic origin. J. Geophys. Res. Atmos. 112, D23S04.

Guo, S., Hu, M., Guo, Q., Zhang, X., Zheng, M., Zheng, J., Chang, C.C., Schauer, J.J., Zhang, R., 2012. Primary sources and secondary formation of organic aerosols in Beijing, China. Environ. Sci. Technol. 46 (18), 9846–9853.

Gustafsson, Ö., Kruså, M., Zencak, Z., Sheesley, R.J., Granat, L., Engström, E., Praveen, P., Rao, P., Leck, C., Rodhe, H., 2009. Brown clouds over South Asia: biomass or fossil fuel combustion? Science 323 (5913), 495–498.

He, H., Wang, Y., Ma, Q., Ma, J., Chu, B., Ji, D., Tang, G., Liu, C., Zhang, H., Hao, J., 2014. Mineral Dust and NOx Promote the Conversion of SO_2 to Sulfate in Heavy Pollution Days. Scientific Reports 4.

Ho, K., Lee, S., Cao, J., Li, Y., Chow, J.C., Watson, J.G., Fung, K., 2006. Variability of organic and elemental carbon, water soluble organic carbon, and isotopes in Hong Kong. Atmos. Chem. Phys. 6 (12), 4569–4576.

Hu, D., Bian, Q., Li, T.W., Lau, A.K., Yu, J.Z., 2008. Contributions of isoprene, monoterpenes, β-caryophyllene, and toluene to secondary organic aerosols in Hong Kong during the summer of 2006. J. Geophys. Res. Atmos. 113, D22206.

Huang, J., Kang, S., Shen, C., Cong, Z., Liu, K., Wang, W., Liu, L., 2010. Seasonal variations and sources of ambient fossil and biogenic-derived carbonaceous aerosols based on ^{14}C measurements in Lhasa, Tibet. Atmos. Res. 96 (4), 553–559.

Huang, R.-J., Zhang, Y., Bozzetti, C., Ho, K.-F., Cao, J.-J., Han, Y., Daellenbach, K.R., Slowik, J.G., Platt, S.M., Canonaco, F., Zotter, P., Wolf, R., Pieber, S.M., Bruns, E.A., Crippa, M., Ciarelli, G., Piazzalunga, A., Schwikowski, M., Abbaszade, G., Schnelle-Kreis, J., Ralf, Z., An, Z., Szidat, S., Baltensperger, U., Haddad, I.E., 2014. High secondary aerosol contribution to particulate pollution during haze events in China. Nature 514 (7521), 218–222.

Kirillova, E.N., Andersson, A., Sheesley, R.J., Kruså, M., Praveen, P.S., Budhavant, K., Safai, P.D., Rao, P.S.P., Gustafsson, Ö., 2013. ^{13}C- and ^{14}C-based study of sources and atmospheric processing of water-soluble organic carbon (WSOC) in South Asian aerosols. J. Geophys. Res. Atmos. 118 (2), 614–626.

Kirillova, E.N., Andersson, A., Han, J., Lee, M., Gustafsson, Ö., 2014. Sources and light absorption of water-soluble organic carbon aerosols in the outflow from northern China. Atmos. Chem. Phys. 14 (3), 1413–1422.

Kleindienst, T.E., Jaoui, M., Lewandowski, M., Offenberg, J.H., Lewis, C.W., Bhave, P.V., Edney, E.O., 2007. Estimates of the contributions of biogenic and anthropogenic hydrocarbons to secondary organic aerosol at a southeastern US location. Atmos. Environ. 41 (37), 8288–8300.

Kroll, J.H., Seinfel, J.H., 2008. Chemistry of secondary organic aerosol: formation and evolution of low-volatility organics in the atmosphere. Atmos. Environ. 42, 3593–3624.

Lee, J.J., Engling, G., Lung, S.-C.C., Lee, K.-Y., 2008. Particle size characteristics of levoglucosan in ambient aerosols from rice straw burning. Atmos. Environ. 42 (35), 8300–8308.

Levin, I., Naegler, T., Kromer, B., Diehl, M., Francey, R.J., Gomez-pelaez, A., Steele, L., Wagenbach, D., Weller, R., Worthy, D.E., 2010. Observations and modelling of the global distribution and long-term trend of atmospheric $^{14}CO_2$. Tellus B 62 (1), 26–46.

Lewandowski, M., Jaoui, M., Offenberg, J.H., Kleindienst, T.E., Edney, E.O., Sheesley, R.J., Schauer, J.J., 2008. Primary and secondary contributions to ambient PM in the midwestern United States. Environ. Sci. Technol. 42 (9), 3303–3309.

Liu, Y., Shao, M., Fu, L., Lu, S., Zeng, L., Tang, D., 2008a. Source profiles of volatile organic compounds (VOCs) measured in China: part I. Atmos. Environ. 42 (25), 6247–6260.

Liu, Y., Shao, M., Lu, S., Chang, C.-C., Wang, J.-L., Fu, L., 2008b. Source apportionment of ambient volatile organic compounds in the Pearl River Delta, China: part II. Atmos. Environ. 42 (25), 6261–6274.

Liu, D., Li, J., Zhang, Y., Xu, Y., Liu, X., Ding, P., Shen, C., Chen, Y., Tian, C., Zhang, G., 2013. The use of levoglucosan and radiocarbon for source apportionment of $PM_{2.5}$ carbonaceous aerosols at a background site in east China. Environ. Sci. Technol. 47 (18), 10454–10461.

Liu, J., Li, J., Zhang, Y., Liu, D., Ding, P., Shen, C., Shen, K., He, Q., Ding, X., Wang, X., Chen, D., Szidat, S., Zhang, G., 2014. Source apportionment using radiocarbon and organic tracers for $PM_{2.5}$ carbonaceous aerosols in Guangzhou, south China: contrasting local-and regional-scale haze events. Environ. Sci. Technol. 48 (20), 12002–12011.

Menon, S., Hansen, J., Nazarenko, L., Luo, Y., 2002. Climate effects of black carbon aerosols in China and India. Science 297 (5590), 2250–2253.

Miyazaki, Y., Kondo, Y., Takegawa, N., Komazaki, Y., Fukuda, M., Kawamura, K., Mochida, M., Okuzawa, K., Weber, R.J., 2006. Time-resolved measurements of water-soluble organic carbon in Tokyo. J. Geophys. Res. Atmos. 111, D23206.

Mohn, J., Szidat, S., Fellner, J., Rechberger, H., Quartier, R., Buchmann, B., Emmenegger, L., 2008. Determination of biogenic and fossil CO_2 emitted by

waste incineration based on $^{14}CO_2$ and mass balances. Bioresour. Technol. 99 (14), 6471–6479.
Paglione, M., Saarikoski, S., Carbone, S., Hillamo, R., Facchini, M., Finessi, E., Giulianelli, L., Carbone, C., Fuzzi, S., Moretti, F., 2014. Primary and secondary biomass burning aerosols determined by proton nuclear magnetic resonance (1H-NMR) spectroscopy during the 2008 EUCAARI campaign in the Po Valley (Italy). Atmos. Chem. Phys. 14 (10), 5089–5110.
Park, S.-S., Jeong, J.-U., Cho, S.-Y., 2012. Group separation of water-soluble organic carbon fractions in ash samples from a coal combustion boiler. Asian J. Atmos. Environ. 6 (1), 67–72.
Pavuluri, C.M., Kawamura, K., Uchida, M., Kondo, M., Fu, P., 2013. Enhanced modern carbon and biogenic organic tracers in northeast Asian aerosols during spring/summer. J. Geophys. Res. Atmos. 118 (5), 2362–2371.
Piazzalunga, A., Bernardoni, V., Fermo, P., Valli, G., Vecchi, R., 2011. Technical note: on the effect of water-soluble compounds removal on EC quantification by TOT analysis in urban aerosol samples. Atmos. Chem. Phys. 11 (19), 10193–10203.
Pöschl, U., 2005. Atmospheric aerosols: composition, transformation, climate and health effects. Angew. Chem. Int. Ed. 44 (46), 7520–7540.
Rao, Z., Chen, Z., Liang, H., Huang, L., Huang, D., 2016. Carbonyl compounds over urban Beijing: concentrations on haze and non-haze days and effects on radical chemistry. Atmos. Environ. 124, 207–216.
Robinson, A.L., Donahue, N.M., Shrivastava, M.K., Weitkamp, E.A., Sage, A.M., Grieshop, A.P., Lane, T.E., Pierce, J.R., Pandis, S.N., 2007. Rethinking organic aerosols: semivolatile emissions and photochemical aging. Science 315 (5816), 1259–1262.
Sang, X.F., Gensch, I., Laumer, W., Kammer, B., Chan, C.Y., Engling, G., Wahner, A., Wissel, H., Kiendler-Scharr, A., 2012. Stable carbon isotope ratio analysis of anhydrosugars in biomass burning aerosol particles from source samples. Environ. Sci. Technol. 46 (6), 3312–3318.
Schichtel, B.A., Malm, W.C., Bench, G., Fallon, S., McDade, C.E., Chow, J.C., Watson, J.G., 2008. Fossil and contemporary fine particulate carbon fractions at 12 rural and urban sites in the United States. J. Geophys. Res. Atmos. 113, D02311.
Shen, R.-Q., Ding, X., He, Q.-F., Cong, Z.-Y., Wang, X.-M., 2015. Seasonal variation of secondary organic aerosol tracers in Central Tibetan Plateau. Atmos. Chem. Phys. 15 (15), 8781–8793.
Song, Y., Zhang, Y., Xie, S., Zeng, L., Zheng, M., Salmon, L.G., Shao, M., Slanina, S., 2006. Source apportionment of PM2.5 in Beijing by positive matrix factorization. Atmos. Environ. 40 (8), 1526–1537.
Sun, Y., Jiang, Q., Wang, Z., Fu, P., Li, J., Yang, T., Yin, Y., 2014. Investigation of the sources and evolution processes of severe haze pollution in Beijing in January 2013. J. Geophys. Res. Atmos. 119 (7), 4380–4398.
Szidat, S., Jenk, T.M., Gäggeler, H.W., Synal, H.-A., Fisseha, R., Baltensperger, U., Kalberer, M., Samburova, V., Wacker, L., Saurer, M., Schwikowski, M., Hajdas, I., 2004. Source apportionment of aerosols by ^{14}C measurements in different carbonaceous particle fractions. Radiocarbon 46, 475–484.
Szidat, S., Ruff, M., Perron, N., Wacker, L., Synal, H.-A., Hallquist, M., Shannigrahi, A.S., Yttri, K., Dye, C., Simpson, D., 2009. Fossil and non-fossil sources of organic carbon (OC) and elemental carbon (EC) in Göteborg, Sweden. Atmos. Chem. Phys. 9 (5), 1521–1535.
Szidat, S., Salazar, G.A., Vogel, E., Battaglia, M., Wacker, L., Synal, H.-A., Türler, A., 2014. ^{14}C analysis and sample preparation at the new Bern laboratory for the analysis of radiocarbon with AMS (LARA). Radiocarbon 56, 561–556.
Uno, I., Sugimoto, N., Shimizu, A., Yumimoto, K., Hara, Y., Wang, Z., 2014. Record heavy $PM_{2.5}$ air pollution over China in January 2013: vertical and horizontal dimensions. Sola 10, 136–140.
Wang, R., Tao, S., Wang, W., Liu, J., Shen, H., Shen, G., Wang, B., Liu, X., Li, W., Huang, Y., 2012. Black carbon emissions in China from 1949 to 2050. Environ. Sci. Technol. 46 (14), 7595–7603.
Wang, L., Wei, Z., Yang, J., Zhang, Y., Zhang, F., Su, J., Meng, C., Zhang, Q., 2014a. The 2013 severe haze over southern Hebei, China: model evaluation, source apportionment, and policy implications. Atmos. Chem. Phys. 14 (6), 3151–3173.
Wang, Y., Zhang, R., Saravanan, R., 2014b. Asian pollution climatically modulates mid-latitude cyclones following hierarchical modelling and observational analysis. Nat. Commun. 5, 3098.
Weber, R.J., Sullivan, A.P., Peltier, R.E., Russell, A., Yan, B., Zheng, M., De Gouw, J., Warneke, C., Brock, C., Holloway, J.S., Atlas, E.L., Edgerton, E., 2007. A study of secondary organic aerosol formation in the anthropogenic-influenced southeastern United States. J. Geophys. Res. Atmos. 112, D13302.
Yang, F., He, K., Ye, B., Chen, X., Cha, L., Cadle, S., Chan, T., Mulawa, P., 2005. One-year record of organic and elemental carbon in fine particles in downtown Beijing and Shanghai. Atmos. Chem. Phys. 5 (6), 1449–1457.
Yu, J.Z., Xu, J., Yang, H., 2002. Charring characteristics of atmospheric organic particulate matter in thermal analysis. Environ. Sci. Technol. 36 (4), 754–761.
Zhang, Y., Perron, N., Ciobanu, V.G., Zotter, P., Minguillón, M.C., Wacker, L., Prévôt, A.S.H., Baltensperger, U., Szidat, S., 2012. On the isolation of OC and EC and the optimal strategy of radiocarbon-based source apportionment of carbonaceous aerosols. Atmos. Chem. Phys. 12 (22), 10841–10856.
Zhang, R., Jing, J., Tao, J., Hsu, S.-C., Wang, G., Cao, J., Lee, C., Zhu, L., Chen, Z., Zhao, Y., 2013a. Chemical characterization and source apportionment of PM 2.5 in Beijing: seasonal perspective. Atmos. Chem. Phys. 13 (14), 7053–7074.
Zhang, Y., Zotter, P., Perron, N., Prévôt, A., Wacker, L., Szidat, S., 2013b. Fossil and non-fossil sources of different carbonaceous fractions in fine and coarse particles by radiocarbon measurement. Radiocarbon 55 (2), 1510–1520.
Zhang, Y., Li, J., Zhang, G., Zotter, P., Huang, R.-J., Tang, J.-H., Wacker, L., Prévôt,, A.S.H., Szidat, S., 2014a. Radiocarbon-based source apportionment of carbonaceous aerosols at a regional background site on Hainan island, South China. Environ. Sci. Technol. 48 (5), 2651–2659.
Zhang, Y., Liu, J., Salazar, G.A., Li, J., Zotter, P., Zhang, G., Shen, R., Schäfer, K., Schnelle-Kreis, J., Prévôt, A.S.H., Szidat, S., 2014b. Micro-scale (μg) radiocarbon analysis of water-soluble organic carbon in aerosol samples. Atmos. Environ. 97, 1–5.
Zhang, Y., Huang, R.-J., El Haddad, I., Ho, K.-F., Cao, J.-J., Han, Y., Zotter, P., Bozzetti, C., Daellenbach, K.R., Canonaco, F., Slowik, J.G., Salazar, G.A., Schwikowski, M., Schnelle-Kreis, J., Abbaszade, G., Zimmermann, R., Baltensperger, U., Prévôt, A.S.H., Szidat, S., 2015. Fossil vs. non-fossil sources of fine carbonaceous aerosols in four Chinese cities during the extreme winter haze episode of 2013. Atmos. Chem. Phys. 15 (3), 1299–1312.
Zhao, P., Dong, F., Yang, Y., He, D., Zhao, X., Zhang, W., Yao, Q., Liu, H., 2013. Characteristics of carbonaceous aerosol in the region of Beijing, Tianjin, and Hebei, China. Atmos. Environ. 71, 389–398.
Zheng, M., Salmon, L.G., Schauer, J.J., Zeng, L., Kiang, C., Zhang, Y., Cass, G.R., 2005. Seasonal trends in $PM_{2.5}$ source contributions in Beijing, China. Atmos. Environ. 39 (22), 3967–3976.
Zotter, P., Ciobanu, V.G., Zhang, Y.L., El-Haddad, I., Macchia, M., Daellenbach, K.R., Salazar, G.A., Huang, R.-J., Wacker, L., Hueglin, C., Piazzalunga, A., Fermo, P., Schwikowski, M., Baltensperger, U., Szidat, S., Prévôt, A.S.H., 2014a. Radiocarbon analysis of elemental and organic carbon in Switzerland during winter-smog episodes from 2008 to 2012-Part 1: source apportionment and spatial variability. Atmos. Chem. Phys. 14, 13551–13570.
Zotter, P., El-Haddad, I., Zhang, Y., Hayes, P.L., Zhang, X., Lin, Y.-H., Wacker, L., Schnelle-Kreis, J., Abbaszade, G., Zimmermann, R., Surratt, J.D., Weber, R., Jimenez, J.L, Szidat, S., Baltensperger, U., Prévôt, A.S.H., 2014b. Diurnal cycle of fossil and nonfossil carbon using radiocarbon analyses during CalNex. J. Geophys. Res. Atmos. 119 (11), 6818–6835.